Destruction of the Tar Present in Syngas by Combustion in Porous Media

ARTICLE *in* ENERGY & FUELS · NOVEMBER 2014

Impact Factor: 2.79 · DOI: 10.1021/ef501807p

5 AUTHORS, INCLUDING:

Mário Costa
University of Lisbon
98 PUBLICATIONS **1,302** CITATIONS
SEE PROFILE

Rafael C. Catapan
Federal University of Santa Catarina
9 PUBLICATIONS **85** CITATIONS
SEE PROFILE

energy&fuels

Article

pubs.acs.org/EF

Destruction of the Tar Present in Syngas by Combustion in Porous Media

T. Carvalho,[†] M. Costa,*[,†] C. Casaca,[†,‡] R. C. Catapan,[§] and A. A. M. Oliveira[∥]

[†]Instituto de Engenharia Mecânica (IDMEC), Mechanical Engineering Department, Instituto Superior Técnico, Universidade de Lisboa, 1049-001 Lisboa, Portugal

[‡]Instituto Superior de Engenharia de Lisboa, Instituto Politécnico de Lisboa, 1549-020 Lisboa, Portugal

[§]Center for Mobility Engineering, Federal University of Santa Catarina, 89218-000 Joinville, Santa Catarina, Brazil

[∥]Mechanical Engineering Department, Federal University of Santa Catarina, 88040-900 Florianópolis, Santa Catarina, Brazil

ABSTRACT: The cleaning of syngas is one of the most important challenges in the development of technologies based on gasification of biomass. Tar is an undesired byproduct because, once condensed, it can cause fouling and plugging and damage the downstream equipment. Thermochemical methods for tar destruction, which include catalytic cracking and thermal cracking, are intrinsically attractive because they are energetically efficient and no movable parts are required nor byproducts are produced. The main difficulty with these methods is the tendency for tar to polymerize at high temperatures. An alternative to tar removal is the complete combustion of the syngas in a porous burner directly as it leaves the particle capture system. In this context, the main aim of this study is to evaluate the destruction of the tar present in the syngas from biomass gasification by combustion in porous media. A gas mixture was used to emulate the syngas, which included toluene as a tar surrogate. Initially, CHEMKIN was used to assess the potential of the proposed solution. The calculations revealed the complete destruction of the tar surrogate for a wide range of operating conditions and indicated that the most important reactions in the toluene conversion are $C_6H_5CH_3 + OH \leftrightarrow C_6H_5CH_2 + H_2O$, $C_6H_5CH_3 + OH \leftrightarrow C_6H_4CH_3 + H_2O$, and $C_6H_5CH_3 + O \leftrightarrow OC_6H_4CH_3 + H$ and that the formation of toluene can occur through $C_6H_5CH_2 + H \leftrightarrow C_6H_5CH_3$. Subsequently, experimental tests were performed in a porous burner fired with pure methane and syngas for two equivalence ratios and three flow velocities. In these tests, the toluene concentration in the syngas varied from 50 to 200 g/Nm^3. In line with the CHEMKIN calculations, the results revealed that toluene was almost completely destroyed for all tested conditions and that the process did not affect the performance of the porous burner regarding the emissions of CO, hydrocarbons, and NO_x.

1. INTRODUCTION

The fast consumption of fossil fuels accompanied by the increase in pollutant emissions that threatens human health and contributes to the greenhouse gases demands new technologies for efficient use of renewable fuels. In this context, biomass is a renewable source that provides sustainable and clean energy production chains. Because of its large spectrum of availability,[1,2] biomass can be used as feedstock for a large number of processes with the advantage that it does not contribute to the atmospheric emissions inventory. Biomass is commonly converted in fuels and/or heat through either thermochemical or biological processes. Within the thermochemical conversion processes, gasification has received great attention recently because of its ability to produce a gaseous fuel that can be used directly for power and/or heat generation and for production of liquid fuels, e.g., by Fischer−Tropsch (FT) synthesis.[3] The composition of the gaseous fuel from biomass or syngas depends upon the design and operating conditions of the gasifier. Major fuel components are H_2, CO, CO_2, CH_4, C_2H_4, and C_2H_6 together with other gases and impurities, such as alkali compounds and tars. The high concentrations of diluents, e.g., CO_2 and N_2, make the syngas a fuel with a low heating value, typically between 4 and 6 MJ/Nm^3, if air is used as the gasifying agent.[4,5] Basu[4] and other investigators[5−8] discussed in detail the design and operation of common types of gasifiers as well as the formation and composition of impurities formed during the gasification of biomass.

The cleaning of the tar present in the syngas is one of the main challenges in the development of technologies based on gasification of biomass. Milne et al.[9] defined tars as the organics produced under thermal or partial oxidation regimes of any organic material that is generally assumed to be largely aromatic, while Moersch et al.[10] considered tars as all aromatic and polyaromatic hydrocarbons present in the syngas. Therefore, tars are composed of hundreds of chemical species with molecular weights between 78 and 300. Once condensed, tars can cause fouling and plugging and damage the downstream equipment.

All gasification processes produce some amount of tar. Tar concentrations vary from 0.05 to 200 g/Nm^3, depending upon the fuel, gasifier, and operating conditions. As an example of the importance of tar removal, the maximum tar concentration allowed for methanol synthesis is 1 mg/Nm^3 and, for FT synthesis, is inferior to 1 ppm.[9,11,12] Valuable reviews on technologies for reduction, removal, and destruction of tars in the syngas through catalytic processes can be found in refs 8 and 13−18. These methods (thermal and catalytic cracking and

Received: August 12, 2014
Revised: November 17, 2014
Published: November 17, 2014

dx.doi.org/10.1021/ef501807p | *Energy Fuels* 2015, 29, 1130−1136

partial combustion) for tar destruction are very attractive because they increase the gasification efficiency through the conversion of the tar to useful gases, such as light hydrocarbons (HCs), without the need for separating the tar from the syngas. In particular, the catalytic cracking of tar is a valuable method because it allows for high conversion rates at moderate temperatures, but the high associated costs and need for regeneration are major disadvantages. The syngas partial combustion also allows for the cracking of the tar into lighter HCs, but a relatively high amount of useful compounds can be found in the flue gas.[18]

In this context, tar destruction through the complete combustion of the syngas might be an interesting alternative. A suitable technology to achieve this may be the combustion of the syngas in porous media. Useful reviews on the various aspects of the combustion in porous media were provided by Howell et al.,[19] Mujeebu et al.,[20] and Wood and Harris,[21] among others, and specific studies on porous burners may be found in refs 22−31. Combustion in porous media has the advantage of increasing the reaction temperature because of its internal heat recirculation. This allows for burning low heating gaseous fuels with relatively large excess air levels, decreasing the emission of HCs, such as those present in tars.

The present study evaluates the destruction of the tar present in the syngas from biomass gasification by combustion in porous media. A gas mixture was used to emulate the syngas, which included toluene as a tar surrogate. Initially, CHEMKIN PRO was used to assess the potential of the proposed solution. Subsequently, experimental tests were performed in a porous burner fired with pure methane and syngas.

2. MATERIALS AND METHODS

2.1. Experimental Setup and Burner Design. Figure 1 presents a schematic of the experimental setup. It includes devices to control

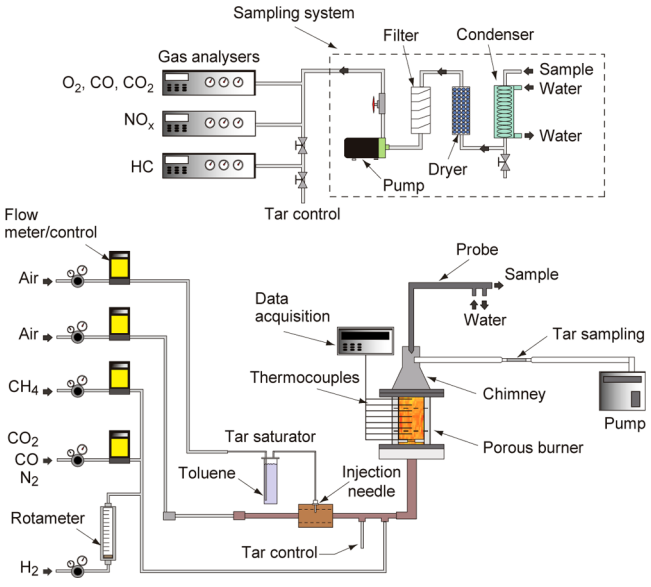

Figure 1. Schematic of the experimental setup.

and measure the flow rates of air, fuel, and tar and to measure temperatures within the porous media and concentrations of the gas species in the flue gas. The air supply was provided through a bottle of pressurized synthetic air and a reducing control valve. The fuel supply system was composed of bottles of pressurized gases and reducing control valves. The gases used include CH_4 (99.8% pure), CO (99.997% pure), CO_2 (99.995% pure), H_2 (99.999% pure), and N_2 (99.999% pure). Mass flow meters connected to precision needle valves were used for measuring and controlling the gaseous fuel flow rates. Toluene was used as a tar surrogate. An air saturator was used to inject toluene in the feed. In the present tests, the toluene concentration in the syngas varied from 50 to 200 g/Nm^3. The mass flow of toluene injected was monitored before being injected in the main air feed.

Figure 2 presents a schematic of the porous burner used, which is described in detail elsewhere.[28,29,31] The burner is made with four

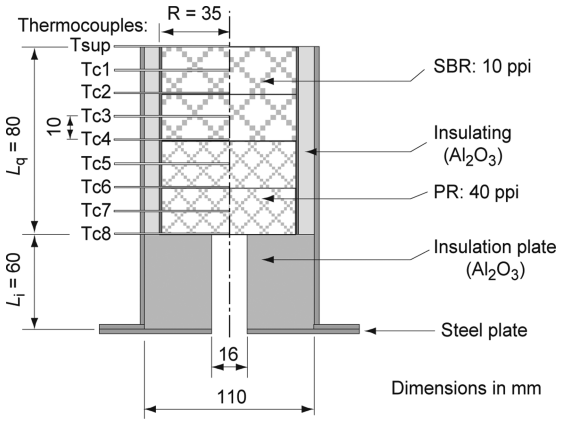

Figure 2. Schematic of the porous burner.

layers of alumina (Al_2O_3) and zirconia (ZrO_2) porous foams, with 80% volumetric porosity, diameter of 70 mm, and thickness of 20 mm. The porous burner is composed by two different regions, the preheating region that is made of two layers of 40 pores per inch (ppi) and the stable-burning region composed of two layers of 10 ppi. An insulation plate and a stainless-steel plate with an injection hole with a diameter of 16 mm were placed upstream of the preheating region.

The temperatures within the porous media were measured using 250 μm diameter wire platinum/platinum/13% rhodium (type R) thermocouples placed in a twin-bore alumina sheath with an external diameter of 1.59 mm. The eight thermocouple beads were positioned in the center of the porous foams and connected to a data acquisition system interfaced with a computer. Because of the thermal equilibrium established between the thermocouple hot junction and gas and solid phases, the measurements provided by this sensor should be understood as a global volume-averaged temperature between the gas and solid phases. Our best estimates have indicated uncertainties in the temperature measurements of less than ±5% of the mean value.

2.2. Experimental Methods. A chimney was placed at the top of the burner to homogenize the flue gas and facilitate sampling (see Figure 1). A portion of the combustion products was sampled with the aid of a water-cooled stainless-steel probe for the measurement of O_2, CO, CO_2, NO_x, and HC concentrations. Before reaching the analyzers, the sample was cleaned and dried. All pipes used in the sampling system were made of polytetrafluoroethylene, which prevented the contamination of the samples. The analyzers included a magnetic pressure analyzer for O_2 measurements, non-dispersive infrared gas analyzers for CO and CO_2 measurements, a flame ionization detector for HC measurements, and a chemiluminescent analyzer for NO_x measurements. Zero and span calibrations with standard mixtures were performed before and after each daily session. The maximum drift in the calibrations was within ±2% of the full scale. In the post-flame region, probe effects are negligible and errors arise mainly from quenching of chemical reactions, sample handling, and analysis. Repeatability of the post-flame gas species concentration data was, on average, within 2% of the mean value.

There are two main methods for the measurement of tars: the cold solvent trapping (CST) and the solid-phase adsorption (SPA) methods. Dufour et al.[32] compared these two methods for the sampling and analysis of tars produced during the pyrolysis of wood.

dx.doi.org/10.1021/ef501807p | Energy Fuels 2015, 29, 1130−1136

The authors concluded that the SPA method presents a number of advantages, namely, an easy chromatography separation, less sampling time, and superior accuracy for the measurement of the light polycyclic aromatic hydrocarbons (PAHs). Brage et al.[33] compared three methods for sampling and analysis of tars, namely, the two methods above and a solid-phase microextraction method, concluding that the solid-phase method with the amino phase can provide much faster and accurate results compared to the CST method. Osipovs[34] also compared the SPA and CST methods. In the SPA method, the author used two different types of adsorbents, one for the volatile organic compounds and other for the heavier compounds. Similar advantages to those found in refs 32 and 33 were reported, and the author[34] also concluded that the SPA method was more suitable for the determination of benzene, toluene, and xylene concentrations than the CST method, with two types of adsorbents. Osipovs[34] also noticed that the CST method is slightly more suitable for the quantification of heavy tar components. Ortiz et al.[35] compared the uncertainties of the SPA and CST methods and concluded that the former method leads to lower uncertainties than the latter method.

In this study, the tar measurements were made using the SPA method. A SKC pump with a flow rate of 100 mL/min was used for sampling. Before reaching the adsorbent, the sample was dried with silica gel. After adsorption, the Tenax adsorbent was analyzed in a gas chromatograph following the automated thermal desorption−gas chromatography−mass spectrometry (ATD−GC−MS) method according to the standard ISO 16000-6:2011. Measurements, both at the inlet and in the flue gas, were repeated 3 times to decrease experimental uncertainty. The estimated uncertainty associated with the SPA method was ±15% of the reported values.

3. CHEMICAL KINETIC MODEL

To assess the potential of the proposed solution for tar destruction, an initial chemical kinetic study was performed with CHEMKIN PRO, using the PREMIX model, developed by Kee et al.[36] The chemical kinetic mechanism employed in this work involves 119 species and 612 elementary reactions. The main syngas mechanism used was developed by Sánchez et al.,[37] while the toluene mechanism was developed by Andrae et al.[38] Additionally, Alzueta et al.[39] established the benzene mechanism that was also used in this study to predict the possibility of benzene formation through the thermal cracking of toluene. The integration of the toluene and benzene mechanisms was established by Andrae et al.[38] In this study, the toluene and benzene mechanisms were integrated in the syngas mechanism.

4. RESULTS AND DISCUSSION

Table 1 presents the composition of the two fuels, named fuels 1 and 2, the equivalence ratios, defined as the ratio of the actual fuel/air ratio to the stoichiometric fuel/air ratio, the flow velocities, and the toluene concentrations used in this study. The composition of fuel 2 was established to represent a typical syngas obtained from gasification of biomass.[29] The burner power varied between 414 W (107 kW/m^2) for fuel 1, with ϕ = 0.4 and flow velocity = 8 cm/s, and 1267 W (321 kW/m^2) for fuel 2, with ϕ = 0.5 and flow velocity = 20 cm/s.

Table 1. Fuel Composition and Equivalence Ratios Used

fuel	composition	ϕ	flow velocity (cm/s)		toluene concentration (g/Nm^3)		
1	100% CH_4	0.5	8	14	50	100	200[a]
2	20% CH_4, 8.9% H_2, 8.9% CO_2, 26.7% CO, and 35.6% N_2	0.5	20[b]				
		0.4					

[a]The saturator did not allow for this concentration for all tested conditions. [b]Tested only for the equivalence ratio of 0.5.

The literature[9] reveals that the highest tar concentration that can be found in the syngas produced in commercial gasifiers is close to 200 g/Nm^3. In this work, toluene ($C_6H_5CH_3$) was used as a tar surrogate with three different concentrations in the syngas, namely, 50, 100, and 200 g/Nm^3. Note, however, that the mass flow rate of toluene was different for each case, ranging from 41 mg/min for fuel 1, with ϕ = 0.5 and flow velocity = 8 cm/s, to 655 mg/min for fuel 2, with ϕ = 0.5 and flow velocity = 20 cm/s.

4.1. Chemical Kinetics Results. In the simulations using CHEMKIN with the PREMIX model, the measured axial temperature profile was prescribed for each condition studied (see Table 1). Figures 3 and 4 show predictions of major and relevant intermediate gas species concentrations, respectively, along the centerline of the porous burner for fuel 2, with 100 g/Nm^3 of toluene, ϕ = 0.5, and flow velocity = 8 cm/s. It can be observed that the main reaction zone is located around a porous burner axial position of 10 mm and that the intermediate gas species in the toluene conversion process include C_6H_6, $OC_6H_4CH_3$, $C_6H_5CH_2$, $C_6H_4CH_3$, C_6H_5CHO, and $HOC_6H_4CH_3$ (note that the radicals H, O, and OH were excluded from Figure 4 for clarity). For ϕ = 0.4 (not shown here), it was observed that the main reaction zone moved downstream to a porous burner axial position of 20 mm and that the intermediate gas species in the toluene conversion process remain essentially the same. The calculations indicate that toluene was completely oxidized for all cases studied.

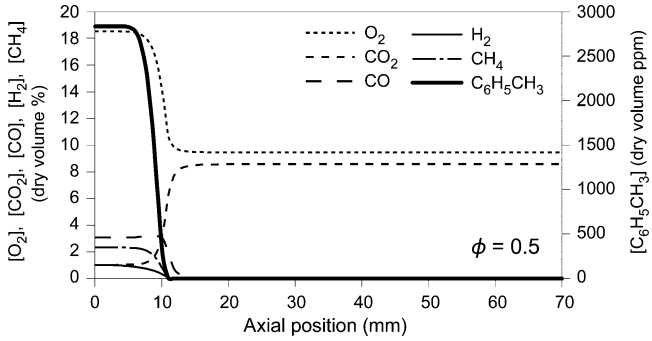

Figure 3. Predictions of major gas species concentrations along the centerline of the porous burner for fuel 2, with 100 g/Nm^3 of toluene, ϕ = 0.5, and flow velocity = 8 cm/s.

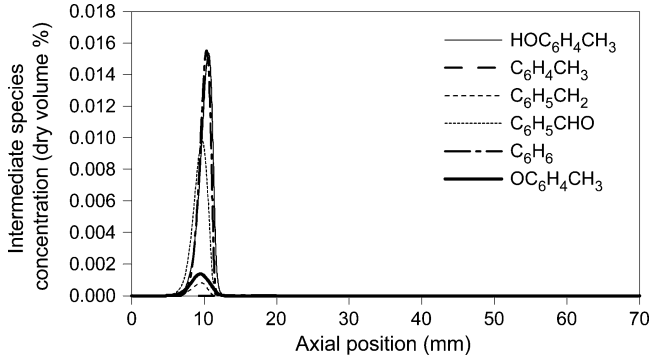

Figure 4. Predictions of relevant intermediate gas species concentrations along the center line of the porous burner for fuel 2, with 100 g/Nm^3 of toluene, ϕ = 0.5, and flow velocity = 8 cm/s.

To gain further insights into the toluene conversion process, Figure 5 shows the toluene absolute rate of production at a

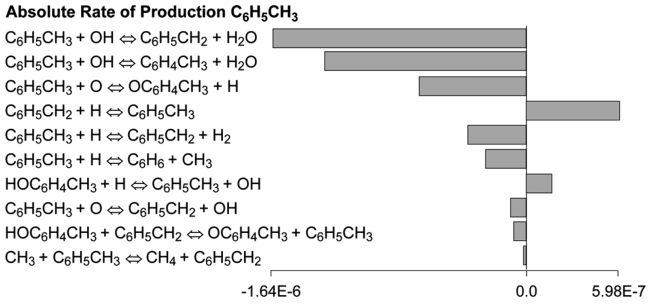

Figure 5. Toluene absolute rate of production at a porous burner axial position of 10 mm for fuel 2, with 100 g/Nm^3 toluene, ϕ = 0.5, and flow velocity = 8 cm/s.

porous burner axial position of 10 mm for fuel 2, with 100 g/Nm^3 of toluene, ϕ = 0.5, and flow velocity = 8 cm/s. Note that Figure 5 represents only the 10 most important reactions for the conversion of the toluene. The set of reactions that have a major contribution to the toluene conversion are

$$C_6H_5CH_3 + OH \leftrightarrow C_6H_5CH_2 + H_2O \quad (1)$$

$$C_6H_5CH_3 + OH \leftrightarrow C_6H_4CH_3 + H_2O \quad (2)$$

$$C_6H_5CH_3 + O \leftrightarrow OC_6H_4CH_3 + H \quad (3)$$

Figure 5 also reveals that formation of toluene can occur through

$$C_6H_5CH_2 + H \leftrightarrow C_6H_5CH_3 \quad (4)$$

Figure 6 shows predictions of the toluene concentration along the centerline of the porous burner for fuel 2, with three

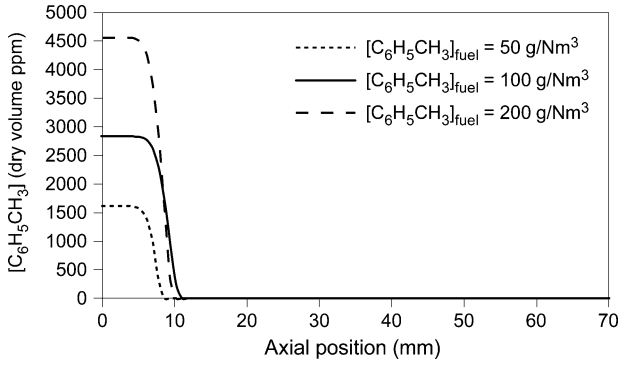

Figure 6. Predictions of the toluene concentration along the centerline of the porous burner for fuel 2, with three concentrations of toluene, ϕ = 0.5, and flow velocity = 8 cm/s.

concentrations of toluene, ϕ = 0.5, and flow velocity = 8 cm/s. The figure reveals that toluene destruction is fully accomplished regardless of the concentration of toluene in the fuel. Moreover, the calculations indicated that the nine most important reactions of the toluene mechanism (see Figure 5) were the same regardless of the concentration of toluene in the fuel.

Similar results (not shown here) were obtained for the remaining test conditions presented in Table 1. All cases examined showed that the toluene addition to the syngas had no impact on the CO, HC, and NO_x emissions, which was confirmed by the experimental results (not shown here).

4.2. Experimental Results. Figure 7 shows the measured temperatures along the centerline of the porous burner for fuels

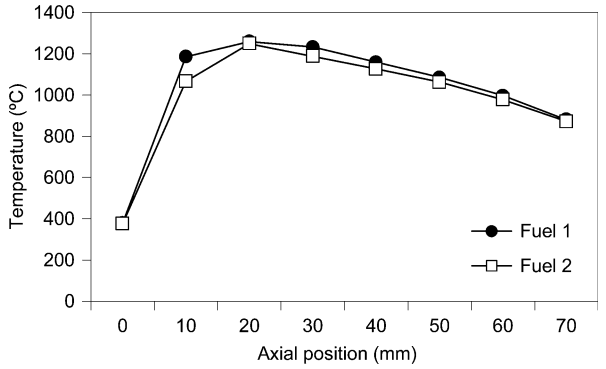

Figure 7. Measured temperatures along the centerline of the porous burner for fuels 1 and 2, with ϕ = 0.5 and flow velocity = 8 cm/s.

1 and 2, with ϕ = 0.5 and flow velocity = 8 cm/s. In both cases, a strong gradient of temperature between 0 and 10 mm, with a temperature peak near to 20 mm, reveal that the flame front is somewhere between 0 and 20 mm. Note that Figures 3 and 4 revealed a flame front located near to 10 mm, when the temperature profile measured for fuel 2 were prescribed in the CHEMKIN simulations. The flame behavior was very similar for both fuels, despite the different mass flow rates of toluene used. For example, the mass flow rate of toluene was 142 mg/min for fuel 1 and 321 mg/min for fuel 2, corresponding in both cases to a toluene concentration of 200 g/Nm^3 in the fuel.

Figure 8 shows the toluene destruction as a function of the toluene concentration in the fuel for fuels 1 and 2, with ϕ = 0.5

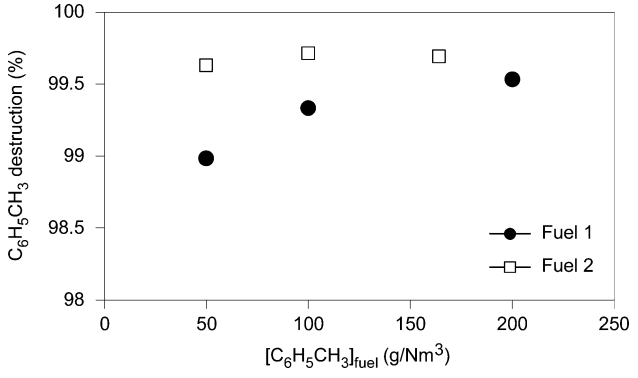

Figure 8. Toluene destruction as a function of the toluene concentration in the fuel for fuels 1 and 2, with ϕ = 0.5 and flow velocity = 8 cm/s.

and flow velocity = 8 cm/s. It can be observed that the toluene destruction is generally higher for fuel 2 than for fuel 1. The temperatures within the porous media (see Figure 7) and, thus, the residence times are similar for all conditions represented in the figure, so that the differences observed in the toluene destruction have to be attributed to the chemical mechanism of the toluene conversion. In fact, the CHEMKIN calculations (not shown here) revealed that the importance of reaction 4 increases and that of reaction 3 decreases when the porous burner is fired with fuel 1 regardless of the toluene concentration in the fuel.

Figure 9 shows the measured temperatures along the centerline of the porous burner for fuel 2, with ϕ = 0.4 and

dx.doi.org/10.1021/ef501807p | Energy Fuels 2015, 29, 1130−1136

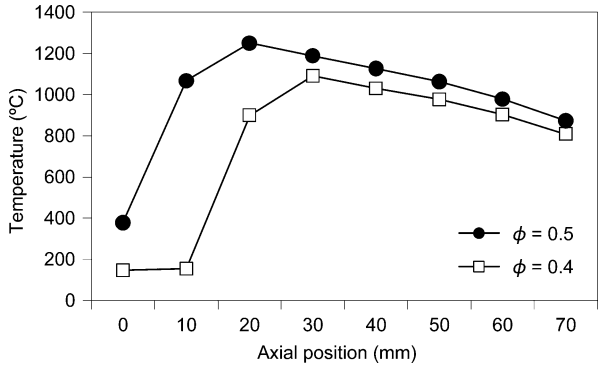

Figure 9. Measured temperatures along the centerline of the porous burner for fuel 2, with ϕ = 0.4 and 0.5 and flow velocity = 8 cm/s.

0.5 and flow velocity = 8 cm/s. In the case of ϕ = 0.4, the measured on-axis temperatures are consistently lower than those measured for ϕ = 0.5. Moreover, the highest temperature for the lower equivalence ratio occurs further downstream, revealing a larger preheating region with lower temperatures close to the injection point of the fuel. Despite this, the axial distance available for the cracking of toluene is similar but with lower temperatures for ϕ = 0.4 than for ϕ = 0.5.

Figure 10 shows the toluene destruction as a function of the toluene concentration in the fuel for fuel 2, with ϕ = 0.4 and 0.5

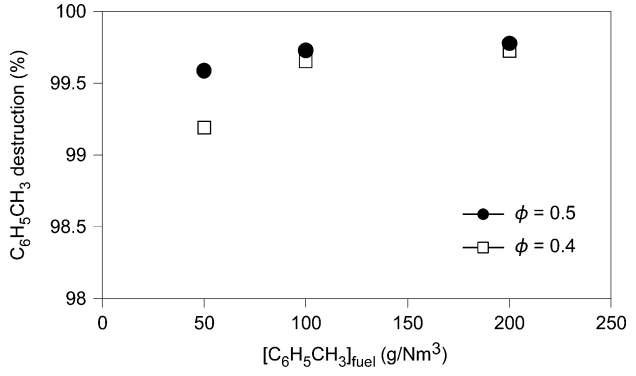

Figure 10. Toluene destruction as a function of the toluene concentration in the fuel for fuel 2, with ϕ = 0.4 and 0.5 and flow velocity = 8 cm/s.

and flow velocity = 8 cm/s. It is seen that the toluene destruction is always lower with the porous burner operating with ϕ = 0.4 than with ϕ = 0.5, which can be attributed to the lower temperatures within the porous media for the former case (see Figure 9). Moreover, in this case, there is a larger region with a lower temperature close to the fuel inlet, which also contributes to the lower toluene conversion observed, despite the longer preheating region. Figure 10 also reveals that the toluene conversion increases for higher mass flow rates of toluene in the syngas probably because of the contribution of the toluene oxidation to the increase in the temperature within the porous burner. The CHEMKIN calculations (not shown here) are consistent with the experimental observations, indicating that the importance of reactions 1−3 increases as the temperature of the porous media increases.

Figure 11 shows the measured temperatures along the centerline of the porous burner for fuel 2, with ϕ = 0.5 and flow velocities = 8, 14, and 20 cm/s. It is seen that, as the flow velocity increases and, thus, the residence time decreases, the

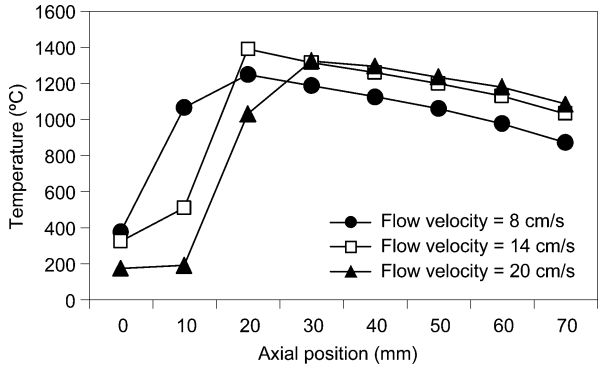

Figure 11. Measured temperatures along the centerline of the porous burner for fuel 2, with ϕ = 0.5 and flow velocities = 8, 14, and 20 cm/s.

flame moves downstream, creating a cooler region close to the injection point but reaching the highest temperatures further downstream. Note that the burner thermal input increases as the flow velocity increases, which allows for the establishment of higher temperatures in the entire burner region located beyond the flame front.

Figure 12 shows the toluene destruction as a function of the toluene concentration in the fuel for fuel 2, with ϕ = 0.5 and

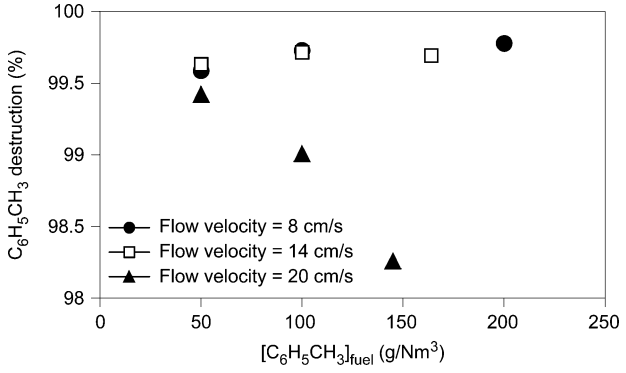

Figure 12. Toluene destruction as a function of the toluene concentration in the fuel for fuel 2, with ϕ = 0.5 and flow velocities = 8, 14, and 20 cm/s.

flow velocities = 8, 14, and 20 cm/s. It is observed that the toluene destruction is similar for the cases with flow velocities = 8 and 14 cm/s, but for the cases with flow velocity = 20 cm/s, the toluene destruction decreases with the increase of the toluene concentration in the fuel. Despite this, the CHEMKIN calculations (not shown here) showed no differences on the main reactions of the toluene mechanism for different flow velocities. Against this background, we can anticipate with reasonable justification that there is a flow velocity or residence time beyond which the effectiveness of the porous burner in oxidizing toluene will reduce significantly.

To conclude, this study revealed that the complete combustion of the syngas in a porous media can be an efficient way for tar destruction; specifically, the present results indicate destruction rates for toluene over 98% regardless of the fuel, equivalence ratio, and flow velocity used.

5. CONCLUSION

The main conclusions of this study are as follows: (1) The CHEMKIN results revealed the complete destruction of toluene for a wide range of operating conditions. The

dx.doi.org/10.1021/ef501807p | Energy Fuels 2015, 29, 1130−1136

calculations indicated that the most important reactions in the toluene conversion are $C_6H_5CH_3 + OH \leftrightarrow C_6H_5CH_2 + H_2O$, $C_6H_5CH_3 + OH \leftrightarrow C_6H_4CH_3 + H_2O$, and $C_6H_5CH_3 + O \leftrightarrow OC_6H_4CH_3 + H$ and that the formation of toluene can occur through $C_6H_5CH_2 + H \leftrightarrow C_6H_5CH_3$. (2) The toluene conversion process did not affect the performance of the porous burner regarding the emissions of CO, HCs, and NO_x. (3) The toluene destruction is generally higher when the porous burner is fired with syngas than with pure methane, which was attributed to the differences in the chemical mechanisms of the toluene conversion in the two cases. (4) The toluene destruction is always lower with the porous burner operating with $\phi = 0.4$ than with $\phi = 0.5$, which was attributed to the lower temperatures within the porous media for the former case. (5) The impact of the flow velocity on the toluene destruction is observed only for velocities well above 14 cm/s, which was attributed to insufficient residence times for effective toluene destruction under those conditions. (6) The porous burner proved to be an efficient way for toluene destruction; the results indicate destruction rates over 98% regardless of the fuel, equivalence ratio, and flow velocity used.

AUTHOR INFORMATION

Corresponding Author

*Telephone: +351218417186. E-mail: mcosta@ist.utl.pt.

Notes

The authors declare no competing financial interest.

ACKNOWLEDGMENTS

This work was supported by Fundação para a Ciência e a Tecnologia (FCT), through IDMEC, under LAETA Pest-OE/EME/LA0022 and PTDC/EME-MFE/116832/2010.

REFERENCES

(1) McKendry, P. Energy production from biomass (part 1): Overview of biomass. *Bioresour. Technol.* **2002**, *83*, 37−46.

(2) Demirbas, A. Biorefineries: Current activities and future developments. *Energy Convers. Manage.* **2009**, *50*, 2782−2801.

(3) McKendry, P. Energy production from biomass (part 2): Conversion technologies. *Bioresour. Technol.* **2002**, *83*, 47−54.

(4) Basu, P. *Biomass Gasification and Pyrolysis—Practical Design and Theory*; Elsevier: Amsterdam, Netherlands, 2010.

(5) Damartzis, T.; Zabaniotou, A. Thermochemical conversion of biomass to second generation biofuels through integrated process design—A review. *Renewable Sustainable Energy Rev.* **2011**, *15*, 366−378.

(6) Panwar, N. L.; Kothari, R.; Tyagi, V. V. Thermochemical conversion of biomass—Eco friendly energy routes. *Renewable Sustainable Energy Rev.* **2012**, *16*, 1801−1816.

(7) McKendry, P. Energy production from biomass (part 3): Gasification technologies. *Bioresour. Technol.* **2002**, *83*, 55−63.

(8) Woolcock, P. J.; Brown, R. C. A review of cleaning technologies for biomass-derived syngas. *Biomass Bioenergy* **2013**, *52*, 54−84.

(9) Milne, T. A.; Evans, R. J.; Abatzoglou, N. *Biomass "Tars": Their Nature, Formation, and Conversion*; National Renewable Energy Laboratory (NREL): Golden, CO, 1998; NREL/TP-570-25357.

(10) Moersch, O.; Spliethoff, H.; Hein, K. R. G. Tar quantification with a new online analyzing method. *Biomass Bioenergy* **2000**, *18*, 79−86.

(11) Beenackers, A. C. M.; Maniatis, K. In *Biomass Gasification and Pyrolysis*; Kaltschmitt, M., Bridgwater, A. V., Eds.; CPL Press: Newbury, U.K., 1997.

(12) Olofsson, I.; Nordin, A.; Söderlind, U. *Initial Review and Evaluation of Process Technologies and Systems Suitable for Cost-Efficient Medium-Scale Gasification for Biomass to Liquid Fuels*; Energy Technology & Thermal Process Chemistry, University of Umeå: Umeå, Sweden, 2005; ETPC Report 05-02.

(13) Anis, S.; Zainal, Z. A. Tar reduction in biomass producer gas via mechanical, catalytic and thermal methods: A review. *Renewable Sustainable Energy Rev.* **2011**, *15*, 2355−2377.

(14) Li, C.; Suzuki, K. Tar property, analysis, reforming and model for biomass gasification—An overview. *Renewable Sustainable Energy Rev.* **2009**, *13*, 594−604.

(15) Dayton, D. *A Review of the Literature on Catalytic Biomass Tar Destruction*; National Renewable Energy Laboratory (NREL): Golden, CO, 2002; NREL/TP-510-32815.

(16) Han, J.; Kim, H. The reduction and control technology of tar during biomass gasification/pyrolysis: An overview. *Renewable Sustainable Energy Rev.* **2008**, *12*, 397−416.

(17) Devi, L.; Ptasinski, K. J.; Janssen, F. J. J. G.; Paasen, S. V. B.; Bergman, P. C. A.; Kiel, J. H. A. Catalytic decomposition of biomass tars: Use of dolomite and untreated olivine. *Renewable Energy* **2005**, *30*, 565−587.

(18) Houben, M. P.; Lange, H. C.; Steenhoven, A. A. Tar reduction through partial combustion of fuel gas. *Fuel* **2005**, *84*, 817−824.

(19) Howell, J. R.; Hall, M. J.; Ellzey, J. L. Combustion of hydrocarbon fuels within porous inert media. *Prog. Energy Combust. Sci.* **1996**, *22*, 121−145.

(20) Mujeebu, M. A.; Abdullah, M. Z.; Bakar, M. Z. A.; Mohamad, A. A.; Muhad, R. M. N.; Abdullah, M. K. Combustion in porous media and its applications—A comprehensive survey. *J. Environ. Manage.* **2009**, *90*, 2287−2312.

(21) Wood, S.; Harris, A. T. Porous burners for lean-burn applications. *Prog. Energy Combust. Sci.* **2008**, *34*, 667−684.

(22) Gao, H.; Qu, Z.; Feng, X.; Tao, W. Combustion of methane/air mixtures in a two-layer porous burner: A comparison of alumina foams, beads, and honeycombs. *Exp. Therm. Fluid Sci.* **2014**, *52*, 215−220.

(23) Rortveit, G. J.; Zepter, K.; Skreiberg, O.; Fossum, M.; Hustad, J. A comparison of low-NO_x burners for combustion of methane and hydrogen mixtures. *Proc. Combust. Inst.* **2002**, *29*, 1123−1129.

(24) Barra, A. J.; Ellzey, J. L. Heat recirculation and heat transfer in porous burners. *Combust. Flame* **2004**, *137*, 230−241.

(25) Keramiotis, C.; Stelzner, B.; Trimis, D.; Founti, M. Porous burners for low emission combustion: An experimental investigation. *Energy* **2012**, *45*, 213−219.

(26) Delalic, N.; Mulahasanovic, Dz.; Ganic, E. N. Porous media compact heat exchanger unit—Experiment and analysis. *Exp. Therm. Fluid Sci.* **2004**, *28*, 185−192.

(27) Talukdar, P.; Mishra, S. C.; Trimis, D.; Durst, F. Heat transfer characteristics of a porous radiant burner under the influence of a 2-D radiation field. *J. Quant. Spectrosc. Radiat. Transfer* **2004**, *84*, 527−537.

(28) Catapan, R. C.; Oliveira, A. A. M; Costa, M. Non-uniform velocity profile mechanism for flame stabilization in a porous radiant burner. *Exp. Therm. Fluid Sci.* **2011**, *35*, 172−179.

(29) Francisco, R. W.; Costa, M.; Catapan, R. C.; Oliveira, A. A. M. Combustion of hydrogen rich gaseous fuels with low calorific value in a porous burner placed in a confined heated environment. *Exp. Therm. Fluid Sci.* **2013**, *45*, 102−109.

(30) Alavandi, S. K.; Agrawal, A. K. Experimental study of combustion of hydrogen-syngas/methane fuel mixtures in a porous burner. *Int. J. Hydrogen Energy* **2008**, *33*, 1407−1415.

(31) Francisco, R. W.; Rua, F.; Costa, M.; Catapan, R. C.; Oliveira, A. A. M. On the combustion of hydrogen-rich gaseous fuels with low calorific value in a porous burner. *Energy Fuels* **2010**, *24*, 880−887.

(32) Dufour, A.; Girods, P.; Masson, E.; Normand, S.; Rogaume, Y.; Zoulalian, A. Comparison of two methods of measuring wood pyrolysis tar. *J. Chromatogr. A* **2007**, *1164*, 240−247.

(33) Brage, C.; Yu, Q.; Chen, G.; Sjöström, K. Use of amino phase adsorbent for biomass tar sampling and separation. *Fuel* **1997**, *76*, 137−142.

(34) Osipovs, S. Comparison of efficiency of two methods for tar sampling in the syngas. *Fuel* **2012**, *103*, 387−392.

(35) Ortiz, I.; Pérez, R. M.; Sánchez, J. M. Evaluation of the uncertainty associated to tar sampling with solid phase adsorption cartridges. *Biomass Bioenergy* **2013**, *57*, 243−248.
(36) Kee, R. J.; Grcar, J. F.; Smooke, M. D.; Miller, J. A. *PREMIX: A Fortran Program for Modeling Steady Laminar One-Dimensional Premixed Flames*; Sandia National Laboratories: Livermore, CA, 1998.
(37) Sánchez, A. L.; Lépinette, A.; Bollig, M.; Liñán, A.; Lázaro, B. The reduced kinetic description of lean premixed combustion. *Combust. Flame* **2000**, *123*, 436−464.
(38) Andrae, J. C. G.; Brinck, T.; Kalghatgi, G. T. HCCI experiments with toluene reference fuels modeled by a semi detailed chemical kinetic model. *Combust. Flame* **2008**, *155*, 696−712.
(39) Alzueta, M. U.; Glarborg, P.; Dam-Johansen, K. Experimental and kinetic modeling study of the oxidation of benzene. *Int. J. Chem. Kinet.* **2000**, *32*, 498−522.